International Journal of Electrical, Electronic and Communication Sciences
ISSN: 2517-9438
Vol:8, No:7, 2014

Phasor Analysis of a Synchronous Generator: A Bond Graph Approach

Israel Núñez-Hernández, Peter C. Breedveld, Paul B. T. Weustink, Gilberto Gonzalez-A

***Abstract*—**This paper presents the use of phasor bond graphs to obtain the steady-state behavior of a synchronous generator. The phasor bond graph elements are built using 2D multibonds, which represent the real and imaginary part of the phasor. The dynamic bond graph model of a salient-pole synchronous generator is showed, and verified viz. a sudden short-circuit test. The reduction of the dynamic model into a phasor representation is described. The previous test is executed on the phasor bond graph model, and its steady-state values are compared with the dynamic response. Besides, the widely used power (torque)-angle curves are obtained by means of the phasor bond graph model, to test the usefulness of this model.

***Keywords*—**Bond graphs, complex power, phasors, synchronous generator, short-circuit, open-circuit,power-angle curve.

I. Introduction

THE synchronous machine has been widely studied and analyzed for many years. The synchronous generator is one of the principal sources of electric energy in the world [1]-[4]. They are designed to be driven by piston engines, steam and gas turbines, as well as hydro and wind turbines.

The sinusoidal analysis using phasors is an easy way to provide insight into the operating point of a synchronous machine without the need to solve differential equations.

At the other hand, the previous work presented on these proceedings [5] describes the basis of the phasor representation in terms of bond graph methodology. A foreknowledge of the material in that paper is suggested.

The present work is described in four sections. After this introduction (Section I), Section II gives a short description of the synchronous generator, and how it is typically modeled in terms of a port-based approach represented by bond graphs. Herein, a sudden short-circuit test is simulated by using the obtained bond graph model as 20-sim® input, and compared with the response of a block diagram model in Simulink®. In Section III, the reduction from a dynamic model to a phasor model is presented. The test described in the previous section is repeated and compared with the steady-state result of the phasor bond graph model. The power-angle and torque-angle curves are obtained through the phasor bond graph model. Section IV presents the conclusions.

Israel Núñez-Hernández, and Peter C. Breedveld are with the Robotics and Mechatronics Group, University of Twente, P.O. Box 217, 7500AE, Enschede, The Netherlands (e-mail: i.nunezhernandez@utwente.nl, P.C.Breedveld@utwente.nl).

Paul B. T. Weustink is with the Controllab Products B.V., Hengelosestraat 500, 7521AN, Enschede, The Netherlands (e-mail: paul.weustink@controllab.nl).

Gilberto Gonzalez-A is with the Faculty of Electrical Engineering, University of Michoacan, Morelia, Michoacán, Mexico (e-mail: gilmichga@yahoo.com).

II. Synchronous Generator

A. Introduction

The synchronous machine is an electromechanical energy converter with a rotating piece named *rotor*, sometimes addressed to as *field*, because its winding generates a constant magnetic field due to a DC injection, and a fixed part named *stator* or *armature*. In the windings of this armature, a rotating magnetic field is generated either by injecting AC (motor) or by turning the rotor carrying a constant field (generator). The energy of this field is mainly contained in the air gap of the machine, and it rotates with the angular frequency of the armature currents, such as in the case of a common three-phase machine. As the adjective 'synchronous' suggests, the rotor rotates at the same frequency as the rotating stator magnetic field during steady-state operation.

The synchronous generator has been modeled mainly by means of Park's transformation [6]. This coordinate transformation, $P(\theta_r)$, removes the dependency of some inductances on the variable rotor position. In other words, the stator variables (natural reference frame f_{abc}) are changed to a reference frame fixed in the rotor (f_{dq0}).

There are different Park's transformations [7], but the power continuity assumption that is inherent to a bond graph junction structure [8] makes mandatory to use a power invariant transformation. Some authors use *dq0* reference frame, and others prefer *qd0* reference frame. The difference lies on the fact that the real variables in one frame are the negative imaginaries variables in the other frame. Due to this fact, sometimes a rotation of $\pi/2$ radians is necessary. For this paper the considered Park transformation is

$$\begin{bmatrix} f_d \\ f_q \\ f_0 \end{bmatrix} = \underbrace{\sqrt{\frac{2}{3}} \begin{bmatrix} \cos\theta_r & \cos(\theta_r - 2\pi/3) & \cos(\theta_r + 2\pi/3) \\ -\sin\theta_r & -\sin(\theta_r - 2\pi/3) & -\sin(\theta_r + 2\pi/3) \\ 1/\sqrt{2} & 1/\sqrt{2} & 1/\sqrt{2} \end{bmatrix}}_{P(\theta_r)} \begin{bmatrix} f_a \\ f_b \\ f_c \end{bmatrix} \quad (1)$$

where the rotor angle is $\theta_r = N_p \int \omega_n dt$, with N_p equal to the number of poles-pairs in the rotor.

We will consider a salient-pole synchronous generator, where two fictitious and orthogonal axis are fixed on the rotor, the direct axis (*d*-axis), and the quadrature axis (*q*-axis). The *d*-axis is chosen in the same direction as the field generated by the field winding *f*. Two damper windings are attached in such a way that one is in line with the *d*-axis (*D* winding), and the

other one (Q winding) is attached to the q-axis.

Assuming that the positive stator current is directed outward of the terminals, and considering that for balanced three-phase systems the 0-axis in (1) is zero, the voltage equations of the synchronous generator [9] may be expressed as

$$\begin{aligned} v_d &= -r_s\, i_d - \omega_r \lambda_q + \tfrac{d}{dt}\lambda_d; & v_f &= r_f\, i_f + \tfrac{d}{dt}\lambda_f \\ v_q &= -r_s\, i_q + \omega_r \lambda_d + \tfrac{d}{dt}\lambda_q; & 0 &= r_D\, i_D + \tfrac{d}{dt}\lambda_D \\ & & 0 &= r_Q\, i_Q + \tfrac{d}{dt}\lambda_Q \end{aligned} \quad (2)$$

The magnetic flux equations are defined by

$$\begin{aligned} \lambda_d &= -L_{ls}\, i_d + L_{md}(-i_d + i_f + i_D); & \lambda_f &= L_{lf}\, i_f + L_{md}(-i_d + i_f + i_D) \\ \lambda_q &= -L_{ls}\, i_q + L_{mq}(-i_q + i_Q); & \lambda_D &= L_{lD}\, i_D + L_{md}(-i_d + i_f + i_D) \\ & & \lambda_Q &= L_{lQ}\, i_Q + L_{mq}(-i_q + i_Q) \end{aligned} \quad (3)$$

where, $\{i_D,\ i_Q\}$, $\{\lambda_D,\ \lambda_Q\}$, $\{r_D,\ r_Q\}$ are the direct and quadrature dampers currents, magnetic fluxes, and resistances; $\{i_d,\ i_q\}$,$\{\lambda_d,\ \lambda_q\}$, $\{v_d,\ v_q\}$ are the stator currents, magnetic fluxes and voltages referred to the rotor reference frame; i_f, v_f, λ_f, r_f are the current, voltage, magnetic flux and resistance in the field winding; r_s is the resistance in the stator winding.

From (2) and (3), we can deduce the synchronous generator electrical scheme,

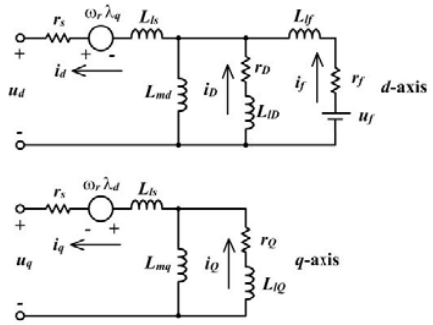

Fig. 1 d-axisand q-axis electrical equivalent circuit

The electromechanical torque is given by

$$T_e = \lambda_d\, i_q - \lambda_q i_d \quad (4)$$

It is important to notice that even though a number of synchronous machine models have been developed, we will be working with the one contained in the IEEE standards [9]. Nevertheless, the names of parameters have been changed in order to make the equations easy to read.

B. Synchronous Generator Bond Graph Model

Due to its nature of a power conserving description of a system, the port-based approach using bond graphs is especially practical when several physical domains have to be modeled within a system simultaneously.

Therefore, the principal advantage of these port-based models over their equivalent circuit counterparts is that they can be directly interconnected with (sub)models from other physical domains in an unified graphical modeling language.

In addition, the port-based approach is in principle an object-oriented approach to modeling. This permits different realizations of an object by directly replacing a portion of it with another bond graph system with a different degree of dynamic details.

Notice the voltage-dependent sources shown in the electrical circuit. These voltage sources, which express the electromotive forces (emf) induced in the stator by the rotor movement, are in fact one side of a 2-port element modulated gyrator MGY. The MGY is a power continuous bond graph element representing a domain transformation [8], [11]. In other words, the gyrator is modeling the electromechanical power exchange.

The advantage of bond graph modeling takes relevance at this point; the electrical circuit does not show a link between the mechanical and the electrical domain. This link is given by (4), where the torque is a function of two electrical variables; therefore, the second side of the MGY is complete. The previous statements explain the two MGY linking the 1-junctions associated with the d- and q- stator currents and the 1-junction associated with angular velocity, ω_r.

At the other hand, the magnetic phenomena in each axis are modeled by means of I-fields [11]. Each field incorporates the constitutive relationship between magnetic fluxes and currents, defined in (3).

In order to represent a constant mechanical angular velocity, a flow source ($S_f : \omega_n$) is added to the mechanical domain.

Then, the equivalent circuit given in Fig. 1 [10], [11] can be converted into the bond graph model in Fig. 2.

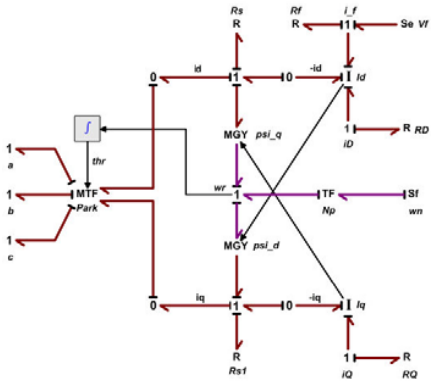

Fig. 2 Bond graph model of synchronous generator

C. Sudden Short-Circuit Test

We will use the parameters of the synchronous generator described by Barakat et al. [12], and we will compare the simulation results provided by these authors in Simulink® with the results of our bond graph model in 20-sim®.

The bond graph model on Fig. 2 needs modification in order to represent the open-circuit test. To achieve this, we will add one switched power junction (SPJ) [13], [14], $X1$, per phase. For more details, including the SIDOPS code of the

SPJ's, the reader is referred to [13], [14].

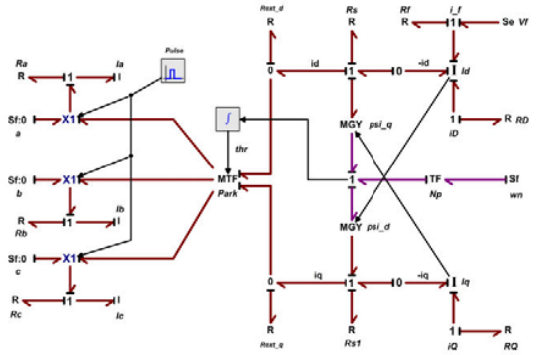

Fig. 3 Sudden short-circuit test in bond graphs

The bond graph model shown in Fig. 3 contains three zero-flow sources $S_f : 0$, which represent the open-circuit state of the machine. One *RL* set circuit is added to each phase, hence with very small parameter values, we are able to simulate a short-circuit test.

At the other hand, two $R : R_{ext}$ elements were also added at the output of *d*- and *q*-*axis*. The value of R_{ext} has to be bigger compared to the rest of resistors, normally around $1\times10^4\,\Omega$ [12]. This was done with the purpose of include the infinite resistance between the ground and the wires in the stator.

Fig. 4 shows the behavior of the voltage at the *phase-a* (u_a) when the generator is working in open-circuit, and at 9 seconds, a short-circuit test is done, and next at 13 seconds, the circuit is open again. Besides, the current at *phase-a* (i_a) is shown in Fig. 5.

We can observe that the responses given by the simulations on 20-sim® are equal to the ones given by Simulink® in [12], therefore, our model is verified.

III. From a Dynamic Model to a Phasor Model

The model in Fig. 3 is represented in a compact way by using the *d*- and *q*-axis circuits in one multibond graph [15] (Fig. 6).

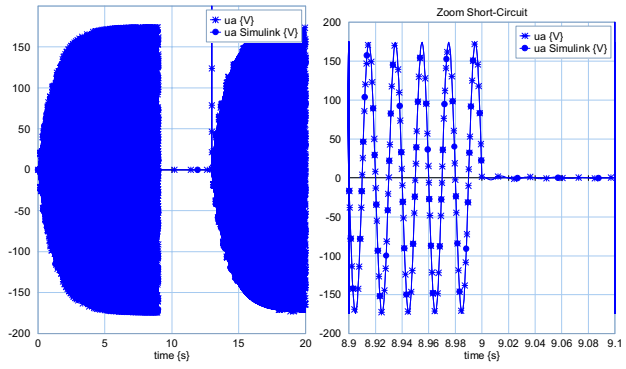

Fig. 4 Stator voltage at *phase-a*

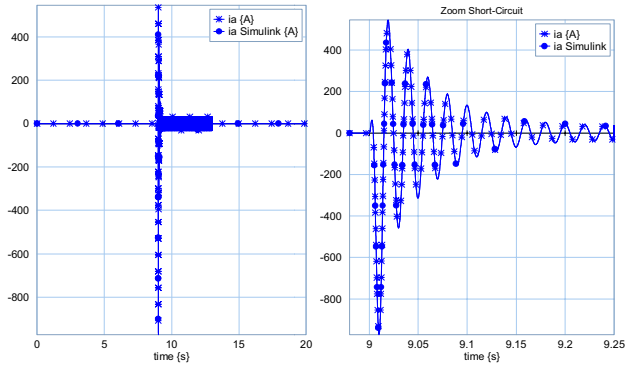

Fig. 5 Stator current at *phase-a*

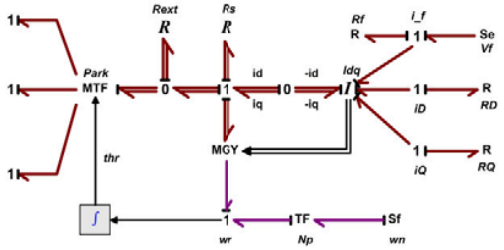

Fig. 6 Synchronous generator vector bond graph

In steady-statemode, the angular velocity of the rotor is equal to the electrical angular velocity, $\omega_r = \omega_e$. This means that the flux linkages of the rotor windings do not change; hence, no current is flowing in the short-circuited damper windings. Also, for balanced steady-state conditions, the variables in the synchronous rotating reference frame are constant; thus $\frac{d}{dt}\lambda_d = \frac{d}{dt}\lambda_q = \frac{d}{dt}\lambda_f = \frac{d}{dt}\lambda_D = \frac{d}{dt}\lambda_Q = 0$. In this way, we can reduce (2) and (3) into

$$\begin{aligned} V_d &= -r_s I_d - \omega_r \psi_q \\ V_q &= -r_s I_q + \omega_r \psi_d \\ V_f &= r_f I_f \end{aligned} \tag{5}$$

$$\begin{aligned} \psi_d &= -L_d I_d + L_{md} I_f \\ \psi_q &= -L_q I_q \end{aligned} \tag{6}$$

The uppercase letters are used to denote steady-state quantities, with RMS value. It is often convenient to express the voltage and flux linkage equations in terms of reactances rather than inductances, $X = \omega_e L$. Likewise, substituting (6) in (5), and using reactances, we have

$$\begin{aligned} V_d &= -r_s I_d + X_q I_q \\ V_q &= -r_s I_q - X_d I_d + X_{md} I_f \\ V_f &= r_f I_f \end{aligned} \tag{7}$$

The torque equation will be discussed later when we obtain the torque curve. We already mentioned that Park's transformation is a change of coordinates into the rotor

reference frame.

In steady-state the synchronous velocity is constant, so, following the reference frame theory [1], we can write

$$F_d = \sqrt{3}F\cos(\theta_r(0)-\theta_e(0)) = \Re\{\sqrt{3}Fe^{j(\theta_r(0)-\theta_e(0))}\}$$
$$F_q = \sqrt{3}F\sin(\theta_r(0)-\theta_e(0)) = -\Re\{j\sqrt{3}Fe^{j(\theta_r(0)-\theta_e(0))}\} \quad (8)$$

where F represents the RMS value of either a voltage, current or magnetic flux. $\theta_r(0)$ is the initial position of the rotor, and $\theta_e(0)$ is the initial angle of the electrical frequency.

As we are working with a balanced system, it is just necessary to represent one phase. The rest of phases may be shifted by $120°$. We can define the phasor for *phase-a* as

$$\vec{F}_a = Fe^{j\theta_e} \quad (9)$$

then we can map F_d and F_q in the complex plane. It is important to note that the rotor reference-frame variables are not phasors; they are real quantities representing the steady-state behavior of the synchronous generator [1]. Thus,

$$\vec{F}_a = \tfrac{1}{\sqrt{3}}\left(F_d + jF_q\right)e^{j\theta_r} = \vec{F}_d + \vec{F}_q \quad (10)$$

where

$$\vec{F}_d = \tfrac{1}{\sqrt{3}}F_d e^{j\theta_r}; \qquad \vec{F}_q = j\tfrac{1}{\sqrt{3}}F_q e^{j\theta_r} \quad (11)$$

Or in matrix representation,

$$\begin{bmatrix}\Re(\vec{F}_a)\\ \Im(\vec{F}_a)\end{bmatrix} = \underbrace{\frac{1}{\sqrt{3}}\begin{bmatrix}\cos\theta_r & -\sin\theta_r\\ \sin\theta_r & \cos\theta_r\end{bmatrix}}_{M}\begin{bmatrix}F_d\\ F_q\end{bmatrix} \quad (12)$$

In order to get the voltage equations of the synchronous machine in phasor representation [7], [16], [17] we substitute (7) in (10), thus

$$\begin{aligned}\vec{V}_a &= \tfrac{1}{\sqrt{3}}\left(-r_s I_d + X_q I_q - jr_s I_q - jX_d I_d + jX_{df} I_f\right)e^{j\theta_r}\\ &= \tfrac{1}{\sqrt{3}}\left(-r_s\left(I_d + jI_q\right) + X_q I_q - jX_d I_d + jX_{df} I_f\right)e^{j\theta_r}\\ &= -r_s\vec{I}_a - jX_q\vec{I}_q - jX_d\vec{I}_d + \vec{E}_q\end{aligned} \quad (13)$$

where $\vec{E}_q = j\tfrac{1}{\sqrt{3}}E_q e^{j\theta_r}$. The term E_q is denominated the *internal emf* of the synchronous generator, and it is given by

$$E_q = X_{md}I_f = \omega_r L_{md} I_f \quad (14)$$

The phasor diagram representing (13) is shown in Fig. 7.

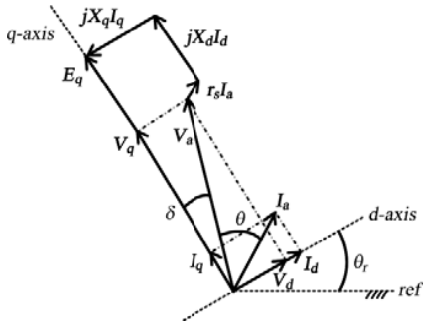

Fig. 7 Synchronous generator phasor diagram

Fig. 7 shows angle δ, called *rotor angle*or *torque angle*. The rotor angle is the electrical angular displacement of the rotor relative to its terminal voltage [1].

The rotor angle is often used to relate torque and speed; we will deal with it in next sections.

Using (12), we may represent (13) in matrix form,

$$\begin{aligned}\vec{V}_a &= \frac{1}{\sqrt{3}}M\left(-\begin{bmatrix}r_s & 0\\ 0 & r_s\end{bmatrix}\begin{bmatrix}I_d\\ I_q\end{bmatrix} - \begin{bmatrix}0 & -X_q\\ X_d & 0\end{bmatrix}\begin{bmatrix}I_d\\ I_q\end{bmatrix} + \begin{bmatrix}0\\ X_{md}I_f\end{bmatrix}\right)\\ &= -R_s\vec{I}_a + \tfrac{1}{\sqrt{3}}M\left(-X_{dq}\vec{I}_{dq} + \vec{E}_{dq}\right)\end{aligned} \quad (15)$$

The phasor bond graph model is obtained using (15),thus

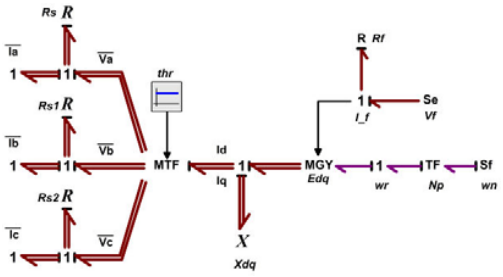

Fig. 8 Phasor bond graph of the synchronous generator

The element $MGY : E_{dq}$ shown in the model depicted in Fig. 8 contains (14) in its electrical side. We will discuss latter the mechanical side. Since we are working on a steady-state, the field current is constant, $I_f = V_f / r_f$, thus we can substitute $R : R_f$ and $Se : V_f$ elements by a block.

A. Steady-State Values of the Sudden Short-Circuit Test Using Phasor Bond Graph Model

In order to simulate these tests, we will add a flow source equal to zero to the model shown in Fig. 8, and a resistor element with a small value per phase to simulate a short-circuit. The model is shown in Fig. 9.

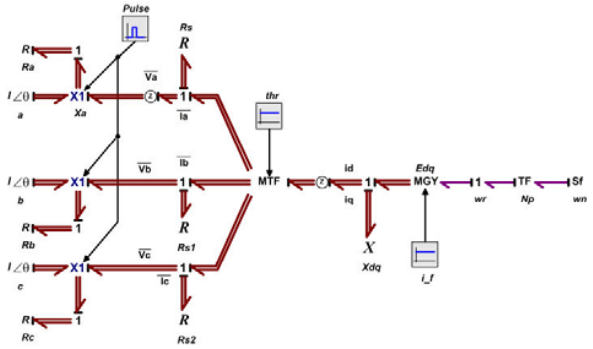

Fig. 9 Sudden short-circuit test in phasor bond graphs

We can appreciate in Fig. 10 the comparison between the voltage at *phase-a* from the dynamic model response done in Simulink®, and the steady-state value of the phasor bond graph model done in 20-sim®.

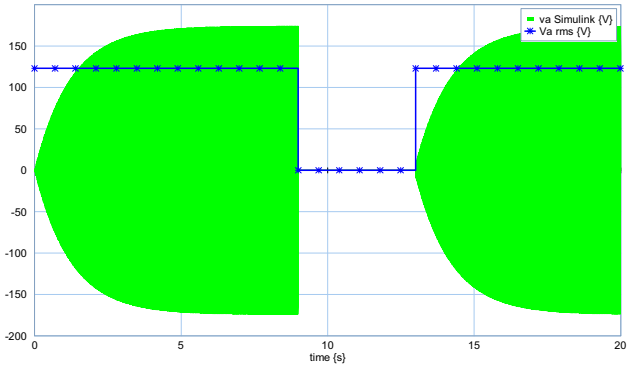

Fig. 10 Comparison between voltage at *phase-a* in steady-state and dynamic response

The same comparison of the current at *phase-a* is shown in Fig. 11.

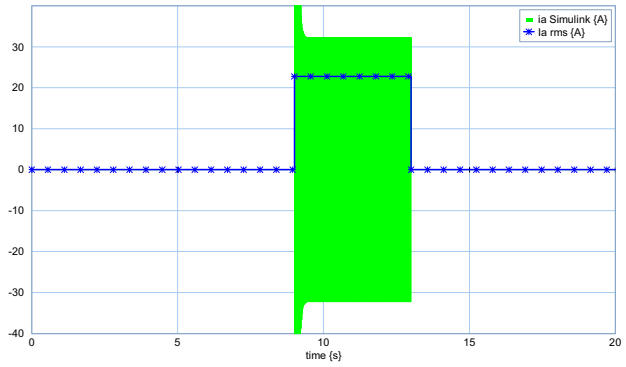

Fig. 11 Comparison between current at *phase-a* in steady-state and dynamic response

Therefore, it is verified that the phasor bond graph model behavior is equal to the machine steady-state expressed in RMS values as it was reached in the dynamic model.

B. Complex Power in the Synchronous Generator

Equation (6) shows the field-winding flux is along the rotor *d*-axis. It produces an emf $\vec{E}_q$ that lags its flux by $\pi/2$ radians, as we can notice in (13). For this reason, the machine emf is primarily along the rotor *q*-axis.

If δ is known, the phasor diagram in Fig. 7 can be constructed. Nevertheless, the position of *q*-axis is not normally known; instead, the terminal conditions of the machine are given. To solve this problem, (13) requires some manipulation.

$$\begin{aligned}\vec{V}_a &= -r_s\vec{I}_a - jX_q\vec{I}_q - jX_d\vec{I}_d + \vec{E}_q - jX_q\vec{I}_d + jX_q\vec{I}_d \\ &= -r_s\vec{I}_a - jX_q\vec{I}_a - j\left(X_d - X_q\right)\vec{I}_d + \vec{E}_q\end{aligned} \tag{16}$$

In order to have a clearer position of the phasor diagram, similar to the one used in [17], (10) will be rotated $\pi/2$ radians in a clockwise direction, thus $\theta_r' = \theta_r - \pi/2$. Consequently, we have

$$\begin{aligned}\vec{F}_a &= \tfrac{1}{\sqrt{3}}\left(F_d + jF_q\right)e^{j\theta_r'} = -j\tfrac{1}{\sqrt{3}}\left(F_d + jF_q\right)e^{j\theta_r} \\ \begin{bmatrix}\Re(\vec{F}_a)\\ \Im(\vec{F}_a)\end{bmatrix} &= \frac{1}{\sqrt{3}}\begin{bmatrix}\cos\theta_r & -\sin\theta_r\\ \sin\theta_r & \cos\theta_r\end{bmatrix}\begin{bmatrix}F_q\\ -F_d\end{bmatrix}\end{aligned} \tag{17}$$

thus, we obtain the phasor diagram shown in Fig. 12.

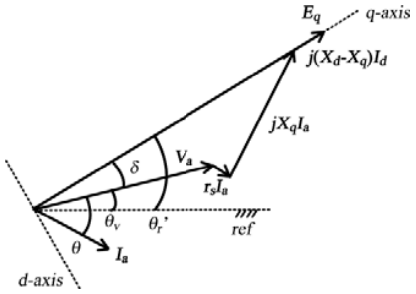

Fig. 12 Phasor diagram representing (16)

We can express (16) in matrix form together with (17), so

$$\begin{aligned}\vec{V}_a &= -R_s\vec{I}_a - \begin{bmatrix}0 & -X_q\\ X_q & 0\end{bmatrix}\vec{I}_a + M\left(\begin{bmatrix}X_d - X_q\\ 0\end{bmatrix}\begin{bmatrix}I_q\\ -I_d\end{bmatrix} + \begin{bmatrix}E_q\\ 0\end{bmatrix}\right) \\ &= -R_s\vec{I}_a - X_q\vec{I}_a + \tfrac{1}{\sqrt{3}}M(X_{dq}\vec{I}_{dq} + E_{dq}) \\ &= -R_s\vec{I}_a - X_q\vec{I}_a + \vec{E}_a\end{aligned} \tag{18}$$

where $\vec{E}_a$ is the internal emf produced by the generator. Once, we have all equations referred to the terminal side of the machine, we can obtain the total real power [18] of the system by using

$$P = V_dI_d + V_qI_q \tag{19}$$

From (7) is neglectedr_s, solving for I_d and I_q, and finally substituting into(19), it yields

$$P = V_d\left(\frac{V_q - X_{df}\, I_f}{-X_d}\right) + V_q\frac{V_d}{X_q} = \left(\frac{1}{X_q} - \frac{1}{X_d}\right)V_d V_q + \frac{V_d E_q}{X_d} \qquad (20)$$

We may express (20) in terms of terminal measurements by using (8); therefore

$$P(V_a) = \underbrace{-\frac{3}{2}V_a^{\,2}\left(\frac{1}{X_q} - \frac{1}{X_d}\right)\sin 2\theta_v}_{\text{reluctance power}} - \underbrace{\frac{\sqrt{3}E_q V_a}{X_d}\sin\theta_v}_{\text{cylindrical power}} \qquad (21)$$

where $\theta_v = \theta_r' - \delta$ is the initial angle at terminal in *phase-a*. It is important to notice that (21) is divided in two terms, the first one is called *reluctance power*, and the second is called *cylindrical power*[18].Equation (21) is a well-known equation to describe the real power[1], [2], [10], [18], [19].

If we wish to know the reactive power [18], then

$$Q = V_q I_d - I_q V_d \qquad (22)$$

We do a similar procedure as in the case of real power, and we obtain an equation in terms of V_a,

$$Q(V_a) = \underbrace{-3V_a^{\,2}\left(\frac{\sin^2\theta_v}{X_q} + \frac{\cos^2\theta_v}{X_d}\right)}_{\text{reluctance power}} + \underbrace{\frac{\sqrt{3}E_q V_a}{X_d}\cos\theta_v}_{\text{cylindrical power}} \qquad (23)$$

In order to obtain the power-angle curves, we will use phasor bond graph model given by (18). We will keep the nominal voltage at the terminal, and we will sweep the load angle, $-\pi \le \theta_v \le \pi$; besides $\theta_r' = 0$ .The phasor bond graph model is depicted in Fig. 13.

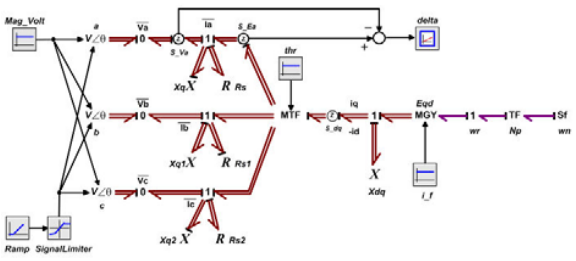

Fig. 13 Phasor bond graph with variable angle load

In Fig. 14 we show the total, cylindrical, and reluctance real power.

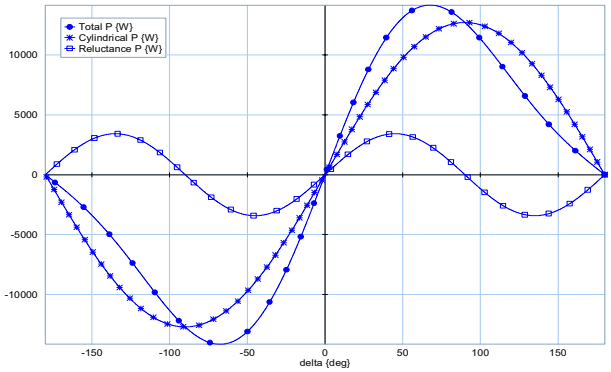

Fig. 14 Real power-angle curves in salient-pole synchronous generator

Similarly, in Fig. 15 we show the reactive powers

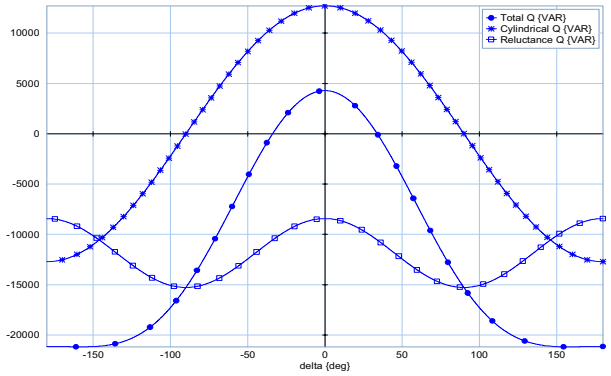

Fig. 15 Reactive power-angle curves in salient-pole synchronous generator

C. Torque-Angle Curve from a Phasor Bond Graph Model

We have obtained the torque equation for the dynamic model. Now, substituting (6) in (4), we get

$$T_e = \lambda_d\, i_q - \lambda_q i_d = (X_q - X_d)I_d I_q + X_{md}\, I_f\, I_q \qquad (24)$$

We introduce (24) inside our $MGY : E_{dq}$ and $MGY : E_{qd}$ elements, respectively on Figs. 9 and 13 in order to complete the mechanical side of the gyrator.

The electrical torque may also be expressed as a function of the real power,

$$T_e = P/\omega_e \qquad (25)$$

The torque-angle curve is compared with the power-angle curve in Fig. 16.

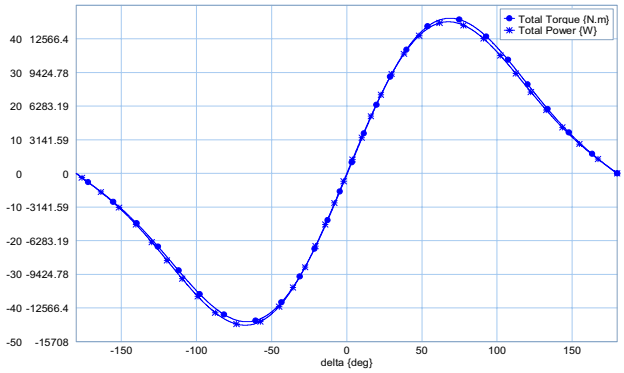

Fig. 16 Torque-angle curve

Notice that in fact the torque and power are scaled each other; nevertheless, they have the same shape. The slightly difference is due to the stator resistance, r_s, was neglected from the power equation.

IV. Conclusion

The dynamic bond graph model of the synchronous generator was verified by comparing the sudden short-circuit responses in 20-sim® with Simulink®.

The necessary steps to reduce a dynamic synchronous generator bond graph model to its phasor bond graph model were shown. The RMS values of stator voltage and current from the phasor bond graph model were compared with the steady-state value of the dynamic model.

In the case of the synchronous generators, the phasor bond graph model has shown an effective way to get torque and power curves, as well as the different angles of voltages, and currents.

Acknowledgment

The authors thank the support given by Dr. Abdallah Barakat with his Simulink® files, and the crew of Controllab®, developers of 20-sim®, for their help in simulation matters. Special thanks to CONACYT (Mexican National Council of Science and Technology) and SEP (Mexican Secretary of Public Education) by the funding of this research.

References

[1] P.C. Krause, O. Wasynczuk, and S.D. Sudhoff, *Analysis of Electric Machinery and Drive Systems*, IEEE Press, Wiley, New York, 2nd edition, 2002.
[2] Ion Boldea, *The Electric Generators Handbook: Synchronous Generators*, Taylor & Francis Group, USA, 2006.
[3] D. Das, *Electrical Power Systems*, New Age International (P) Limited, New Delhi, 2006.
[4] Gilbert M. Masters, *Renewable and Efficient Electric Power Systems*, John Wiley & Sons, USA, 2004.
[5] Israel Núñez-Hernández, Peter C. Breedveld, Paul B. T. Weustink, Gilberto Gonzalez-A, "Analysis of Electrical Networks Using Phasors: A Bond Graph Approach", Paper presented at the International Conference on Electric Machines and Drive Systems, 18-19 July, 2014, Oslo. (in press).
[6] R. H. Park, "Two-Reaction Theory of Synchronous Machines-Generalized Method of Analysis", Part I, AIEE Transactions, Vol. 48, July 1929, pp. 716-727.
[7] P. M. Anderson, A. A. Fouad, *Power System Control and Stability*, 2nd edition, John Wiley & Sons, USA, 2003.
[8] D. Karnopp, "Power-conserving transformation: Physical interpretations and applications using bond graphs", J. Franklin Inst., Vol. 288 (Sept. 1969), pp. 175–201
[9] IEEE Std 1110-2002(R2007), IEEE Guide for Synchronous Generator Modeling Practices and Applications In Power System Stability Analyses, IEEE Power Engineering Society, 2007.
[10] D. Sahm, "A Two-Axis, Bond Graph Model of the Dynamics of Synchronous Electrical Machines", Journal of the Franklin Institute, 1979, vol. 308, No. 3, pp. 205-218.
[11] Wolfgang Borutzky, *Bond Graphs: A Methodology for Modelling Multidisciplinary Dynamic Systems*, Springer, London, 2010.
[12] Abdallah Barakat, Slim Tnani, Gérard Champenois, Emile Mouni, "Analysis of synchronous machine modeling for simulation and industrial applications", Elsevier, Simulation Modelling Practice and Theory 18, 2010, pp. 1382–1396.
[13] Junco, S., Diéguez, G., Ramírez, F., "On commutation modeling in Bond Graphs", Proc. Int. Conf. on Bond Graph Modeling and Simulation, San Diego, 2007, pp. 12-19.
[14] A. C. Umarikar and L. Umanand. 2005, "Modelling of switching systems in bond graphs using the concept of switched power junctions", Journal of The Franklin Institute, 342, pp 131-147.
[15] S. Junco. "Real- and complex-power bond graph modeling of the induction motor". In Proceeding of the International Conference on Bond Graph Modeling and Simulation, pages 323–328, San Francisco, 1999.
[16] Jan Machowski, Janusz W. Bialek, James R. Bumby, *Power System Dynamics: Stability and Control*, 2nd edition, John Wiley & Sons, Great Britain, 2008.
[17] IEEE Std 115™-2009, *IEEE Guide for Test Procedures for Synchronous Machines*, IEEE Power Engineering Society, 2009.
[18] Stephen J. Chapman, *Electric Machinery Fundamentals*, 4th edition, McGraw-Hill, New York, 2005.
[19] Mohamed E. El-Hawary, *Electrical Power Systems*, John Wiley & Sons, New York, 1995.